GEOPHYSICAL RESEARCH LETTERS, VOL. 24, NO.8, PAGES 893-896, APRIL 15, 1997

Tidally induced Sagnac signal in a ring laser

Volker Rautenberg, Hans-Peter Plag

Institut für Geophysik der Christian-Albrechts-Universität zu Kiel, Germany

Michael Burns, Geoffrey E. Stedman

Dept. of Physics and Astronomy, University of Canterbury, Christchurch, New Zealand

Hans-Ulrich Jüttner

Institut für Geophysik der Christian-Albrechts-Universität zu Kiel, Germany

Abstract. The Earth rotation vector is an integral dynamical quantity of the Earth system, with Earth rotation variations depending on the overall dynamics of the Earth system at all time scales. New observations of Earth rotation variations with a precision better than 10^{-9} of the Earth rotation would contribute to the understanding of many geophysical phenomena. High precision short–term observations of the projection of the Earth rotation vector $\mathbf{\Omega}_E$ on the area vector $\mathbf{A}$ of a ring laser are now possible. Tidally induced Sagnac effects are due to changes in the ring geometry (areal strain and perimeter variations), changes in the normal vector of the ring laser plane (tilt), and the vorticity of the Earth's tidal deformations. Here we estimate the latitude-dependent effect of the Earth's body tide deformations due to vorticity and tilt. At mid-latitudes, the vorticity $\delta\mathbf{\Omega}$ is of the order $8 \cdot 10^{-8}\Omega_E$, but because it is in the local horizontal plane, it is not detectable by a horizontal ring. The Sagnac effect due to tidal tilt for a horizontal ring at mid-latitudes is of the order of $4 \cdot 10^{-8}$ of the Earth rotation effect. Thus, the tidal signal is of an order of magnitude where it may be used for validation of existing and future ring lasers.

Introduction

Earth rotation variations are caused by angular momentum exchange between the solid Earth and other parts of the Earth system or other celestial bodies, as well as by changes in the moment of inertia associated, for example, with mass movements on the surface or inside the solid Earth [see e.g. *Lambeck*, 1988; *Hide and Dickey*, 1991]. Earth rotation variations are of paramount interest for understanding the dynamics of the Earth system on time scales ranging from minutes up to million of years. On the time scales directly accessible by modern measurements, more precise observations of polar motion (PM) and length of day (LOD) would contribute to the understanding of a number of geophysical phenomena such as free oscillations of the Earth, the rheology of the Earth's mantle, and the Earth's rotational eigenmodes [see, e.g., *Dehant et al.*, 1993].

Paper number 97GL00760.
0094-8534/97/97GL-00760$05.00

Currently the most precise PM and LOD observations are obtained with space-geodetic methods with the most promising one in terms of temporal resolution and accuracy being Very Long Baseline Interferometry (VLBI). For daily resolutions, precisions are of the order of $0.5 - 2.5 \cdot 10^{-9}$ in PM and $5 \cdot 10^{-10}$ in LOD [*Herring and Dong*, 1994]. However, VLBI is a rather complex method requiring vast resources and international cooperation to achieve highest possible accuracies. The VLBI data processing introduces a time delay of five days between observation and PM and LOD availability. Therefore, developing an alternative technique with its own advantages and disadvantages and with data being more promptly available would be an important step forward.

Ring lasers are a promising technique, which eventually may provide highly accurate determinations of rotation with high temporal resolution at a given point. A major problem of ring lasers is the drift. In a combination of VLBI and ring lasers, VLBI can be used to remove the drift, and this would allow to study the Earth rotation spectrum at the up-to-now poorly understood hour-to-days periods.

A locally stationary ring laser senses the Sagnac effect [*Anderson et al.*, 1994], i.e. a beat frequency f between counterpropagating electromagnetic beams:

$$f = \frac{4\,\mathbf{A} \cdot \mathbf{\Omega}}{\lambda P} \tag{1}$$

where $\mathbf{A} = A\,\mathbf{n}$ is the area vector of the ring, P its perimeter, λ the wavelength of the light, $\mathbf{\Omega}$ the local angular velocity relative to an inertial frame, and $\mathbf{n}$ the normal vector of the ring laser plane. A precision of the order of 10^{-6} has been attained for the measurement of the Earth–rotation induced beat frequency [*Stedman et al.*, 1995]. A better precision is expected in a second-generation large ring laser (C-II) [*Anderson et al.*, 1994; *Bilger et al.*, 1995] which is now under test and which will significantly increase the geophysical relevance of the ring laser measurements.

The main limitation for measurements of Earth rotation variations by ring lasers will most likely be due to local effects. Therefore, it is of interest to study the relation of Earth rotation variations and the local rotation observed by a ring laser. These effects are of interest not only for ring lasers and all other gyro-based observation techniques, but also for the broader field of tidal tilt or gravity measurements, as well

as other techniques for Earth rotation measurements. In all these applications local site effects gain increasing importance.

Local variations of the Sagnac signal

Assuming for each of the quantities $\mathbf{\Omega}$, $\mathbf{n}$, A, and P a perturbation (e.g., $\mathbf{\Omega} = \mathbf{\Omega}_0 + \delta\mathbf{\Omega}$), for a ring laser with $\mathbf{A}$ not perpendicular to $\mathbf{\Omega}$[1], the relative variation in the beat frequency is given to first order by

$$\frac{\delta f}{f} = \frac{\delta\mathbf{\Omega}\cdot\mathbf{n}_0}{\mathbf{\Omega}_0\cdot\mathbf{n}_0} + \frac{\mathbf{\Omega}_0\cdot\delta\mathbf{n}}{\mathbf{\Omega}_0\cdot\mathbf{n}_0} + \frac{\delta A}{A_0} - \frac{\delta P}{P_0} . \qquad (2)$$

Here we will concentrate on the first two terms of the right hand side of eq. (2), namely the *vorticity* term δf_Ω and the *projection* term $\delta f_\mathbf{n}$ arising from $\delta\mathbf{\Omega}$ and $\delta\mathbf{n}$, respectively. These two terms are independent of specific features of the ring laser and its coupling to the Earth's surface. Moreover, they are also relevant to all other gyroscope-based Earth rotation monitoring systems.

It is convenient to split $\delta\mathbf{\Omega}$ into a global part arising from variations in the (global) rotation vector itself and a local part due to, for example, rotation of the local surface. Thus,

$$\delta\mathbf{\Omega} = \delta\mathbf{\Omega}_{\mathrm{glob}} + \delta\mathbf{\Omega}_{\mathrm{loc}} , \qquad (3)$$

with this separation depending on the reference frame used to describe the local effects. We will first consider $\delta\mathbf{\Omega}_{\mathrm{loc}}$ in a suitable reference frame and then comment on the remaining $\delta\mathbf{\Omega}_{\mathrm{glob}}$ not accounted for by $\delta\mathbf{\Omega}_{\mathrm{loc}}$.

An area $\mathbf{A}_\mathrm{S} = A_\mathrm{S}\,\mathbf{n}_\mathrm{S}$ at the Earth's surface or inside the Earth changes due to a deformation field $\mathbf{u}(\mathbf{r},t)$ up to first order in $\mathbf{u}$ as

$$\delta\mathbf{A}_\mathrm{S} = (\nabla\times\mathbf{u})\times\mathbf{A}_\mathrm{S} - \nabla\times(\mathbf{u}\times\mathbf{A}_\mathrm{S}) . \qquad (4)$$

This may be decomposed into an areal variation

$$\delta A_\mathrm{S} = A_\mathrm{S}\,\mathbf{n}_\mathrm{S}\cdot\big(\nabla\times(\mathbf{n}_\mathrm{S}\times\mathbf{u})\big) \qquad (5)$$

and the variation of the normal vector

$$\delta\mathbf{n}_\mathrm{S} = \mathbf{n}_\mathrm{S}\times\big(\mathbf{n}_\mathrm{S}\times\nabla(\mathbf{n}_\mathrm{S}\cdot\mathbf{u})\big) . \qquad (6)$$

A ring laser on the Earth's surface rotates according to the Earth rotation and local vorticity and changes its normal according to the change in the normal vector of the Earth's surface. Thus, for a ring laser with normal $\mathbf{n}_0$ mounted on the Earth's surface with the local normal $\mathbf{n}_\mathrm{S}$ we have

$$\delta\mathbf{\Omega}_{\mathrm{loc}} = \tfrac{1}{2}\,\nabla\times\dot{\mathbf{u}} , \quad \delta\mathbf{n} = \mathbf{n}_0\times\big(\mathbf{n}_\mathrm{S}\times\nabla(\mathbf{n}_\mathrm{S}\cdot\mathbf{u})\big) . \qquad (7)$$

Note that δA in eq. (2) is equal to δA_S given in eq. (5) only if the ring laser is perfectly coupled and parallel to the local Earth's surface. Even for a perfectly decoupled ring laser changes of the gravity field induce changes in A and P, depending on the elastic properties of the ring laser.

Deformations of the Earth's surface are caused by exogenic and endogenic processes. Endogenic deformations are generally small (of the order of mm/yr with rotations of the order of a degree per 10^6 a) or episodic in time and local in space (e.g., earthquakes). Seismic oscillations have periods of less than one hour and are not considered here. Exogenic deformations result from tidal forces and surface loading and traction. On time scales of days to years, the primary exogenic deformations of the Earth's surface are forced by the Earth's body tides and tidal and non-tidal (oceanic, hydrological and atmospheric) loading. Tidal effects dominate at the level of $\geq 10^{-8}\Omega_\mathrm{E}$; other geophysical sources of vorticity are at the level of $10^{-8} - 10^{-9}\Omega_\mathrm{E}$ [*Bilger*, 1984].

The computation of exogenic deformations of the Earth generally are based on the momentum balance of an elastic or viscoelastic continuum, taking into account the gravitational effects of the deformations [e.g., *Wilhelm*, 1986]. For spherically symmetric, non-rotating, elastic, isotropic (SNREI) Earth models, the resulting equations of motion can be solved separately for spheroidal and toroidal forcing. These models do not account for the effect of the Earth's rotation and the induced ellipticity on the deformations; however, these effects are of an order of less than 1 % [*Wang*, 1991]. The Earth's tidal potential described in the next section is purely spheroidal and for spherically symmetric models results in purely spheroidal deformations. Similarly, surface loads produce spheroidal deformations, only. For Earth body tides, the coupling of spheroidal and toroidal solutions for laterally heterogeneous or rotating models are, however, small [$\approx$ 1 %, *Wang*, 1991], and can be neglected here. Based on Love numbers [see e.g., *Wilhelm*, 1986], the computation of $\delta\mathbf{\Omega}_{\mathrm{loc}}$ and $\delta\mathbf{n}$ is easily carried out and is described below. At coastal locations, typically 90 % of the tidal tilt (i.e., $\delta\mathbf{n}$) are contributed by ocean tide loading [*Farrell*, 1972] with this loading effect rapidly decreasing with distance to the coast. However, the computation of $\delta\mathbf{\Omega}_{\mathrm{loc}}$ for ocean tidal loading is more complex due to the necessary convolution of a Green's function with an ocean tidal model and will be discussed elsewhere.

Tidal deformations

At an arbitrary position $\mathbf{r}$ and epoch t the Earth is subjected to astronomical tidal accelerations $\mathbf{a}(\mathbf{r},t)$ which are defined as the difference of extra-terrestrial gravitational accelerations $\mathbf{a}_{\mathrm{et}}(\mathbf{r},t)$ and the Earth's uniform orbital acceleration $\mathbf{a}_{\mathrm{et}}(\mathbf{r}_0,t)$

$$\mathbf{a}(\mathbf{r},t) = \mathbf{a}_{\mathrm{et}}(\mathbf{r},t) - \mathbf{a}_{\mathrm{et}}(\mathbf{r}_0,t) \qquad (8)$$

where $\mathbf{r}_0$ denotes the position of the geocentre. The tidal acceleration is expressed as the gradient of a scalar potential, the so-called tide generating potential (TGP) $\phi = \phi(\mathbf{r},t)$, with $\phi(\mathbf{r}_0,t) \equiv 0$. A typical representation of the TGP utilizes the *harmonic development* [see e.g., *Hartmann and Wenzel*, 1994] which gives a finite set of *partial tides* of harmonic degrees $n \geq 2$ and orders m ($0 \leq m \leq n$). m indicates the tidal band (0: long-period, 1: diurnal, 2: semi-diurnal, etc.), with each band having a large number of partial tides with slightly different frequencies. Although the physical TGP is real-valued, it is convenient to use a complex form $\phi(\mathbf{r},t) = \sum_{nmk}\phi_{nmk}(\mathbf{r},t)$ (with $-n \leq m \leq n$), where the k-th partial tide of the (n,m)-group is given by

$$\phi_{nmk}(\mathbf{r},t) = D\,C_{nmk}\left(\tfrac{r}{R_t}\right)^n Y_{nm}(\vartheta,\lambda)\,e^{i(\omega_{nmk}t-\delta_{nmk})} . \qquad (9)$$

[1]The case $\mathbf{A}\perp\mathbf{\Omega}$ is not of interest here since if $\mathbf{A}$ is nearly perpendicular to $\mathbf{\Omega}$ then the two counterpropagating beams would be locked to each other and there would be no Sagnac effect at all.

Here the position $\mathbf{r}$ is given in geocentric spherical coordinates (radius r, colatitude ϑ, and longitude λ), D is the Doodson constant [see e.g., *Ducarme*, 1989], R_t the radius of reference of the TGP model, C_{nmk} the amplitude, ω_{nmk} the circular frequency, δ_{nmk} the phase, and Y_{nm} the spherical harmonics.

The response $\mathbf{u}(\mathbf{r},t) = \sum_{nmk} \mathbf{u}_{nmk}(\mathbf{r},t)$ of an SNREI Earth model with radius R_e to periodic forcing by partial tides may be expressed by the dimensionless, radius-dependent Love-Shida numbers $h_n(r)$ for radial and $\ell_n(r)$ for horizontal displacements[2] [*Wilhelm*, 1986] with

$$\mathbf{u}_{nmk}(\mathbf{r},t) = \frac{1}{g}\left[h_n(r)\mathbf{e}_r + \ell_n(r)\nabla_o\right]\phi_{nmk}(R_e,\vartheta,\lambda,t) \quad (10)$$

where g is the gravitational acceleration at the Earth's surface, $\mathbf{e}_r$ the radial unit vector, and ∇_o the spherical nabla operator, $\nabla_o \equiv r\,[\nabla - \mathbf{e}_r(\mathbf{e}_r\cdot\nabla)]$. Hence

$$\nabla\times\mathbf{u}_{nmk}(\mathbf{r},t)\Big|_{r=R_e} = \frac{2}{g}\frac{\ell_n - h_n}{R_e}\,\mathbf{e}_r\times\nabla_o\phi_{nmk}(R_e,\vartheta,\lambda,t) \quad (11)$$

where we have used the fact that the surface of the Earth remains free of horizontal stress for deformations due to body tide or surface loading, which leads to

$$\frac{d\ell_n}{dr}\Big|_{r=R_e} = \frac{\ell_n(R_e) - h_n(R_e)}{R_e}\,. \quad (12)$$

As a result, the vorticity and the variation of the normal as given in Eq. (7) have the form

$$\delta\boldsymbol{\Omega}_{\rm loc} = \frac{1}{g}\sum_{nmk}\frac{\ell_n - h_n}{R_e}\,\mathbf{e}_r\times\nabla_o\dot{\phi}_{nmk}, \quad (13)$$

$$\delta\mathbf{n} = \frac{1}{g}\sum_{nmk}\mathbf{n}_0\times\Big(\mathbf{n}_S\times\nabla[h_n(\mathbf{n}_S\cdot\mathbf{e}_r) + \ell_n(\mathbf{n}_S\cdot\nabla_o)]\Big)\,\phi_{nmk}\,. \quad (14)$$

It should be noted that as a consequence of the spheroidal forcing $\delta\boldsymbol{\Omega}_{\rm loc}$ is perpendicular to $\mathbf{e}_r$, therefore, a horizontal ring laser will not sense this signal. On the other hand, $\delta\mathbf{n}$ is perpendicular to $\mathbf{n}_0$ and a ring laser with a normal not aligned with $\boldsymbol{\Omega}_E$ will be sensitive to tilting.

Sagnac contribution from vorticity

Since $\delta\boldsymbol{\Omega}_{\rm loc}$ is perpendicular to $\mathbf{e}_r$, the vorticity contribution δf_Ω to the Sagnac frequency vanishes for a horizontal ring laser with $\mathbf{n}_0 = \mathbf{e}_r$. Currently, large ring lasers are confined to horizontal mounts in order to avoid serious technical problems expected for tilted ring lasers. Nevertheless, an equatorial mount, i.e. $\mathbf{n}_0 = (1/\Omega)\,\boldsymbol{\Omega}$, has already been under discussion in order to maximize the Sagnac signal.

To demonstrate the effect of vorticity, we have chosen a locally vertical mount with $\mathbf{n}_0 = \mathbf{n}_S = \mathbf{e}_\vartheta$ (for example, a vertical ring laser fixed to a vertical wall of a cavity with the normal pointing south). For a ring laser with $\mathbf{n}_0 = (1/\Omega)\,\boldsymbol{\Omega}$, the effect would simply be diminished by a factor of $\sin\vartheta$ compared to our example. Fig. 1 gives $\delta f_\Omega/f$ for a vertical ring laser at Christchurch, New Zealand, where the (horizontal) ring laser C-I is located [*Stedman et al.*, 1995]. For the strongest semi-diurnal tides *M2, N2, S2* (with $m = 2$) and diurnal tides *K1, K1M, O1, P1* ($m = 1$), at this location $\delta f_\Omega/f$ is of the order of $8\cdot10^{-8}$ and $4\cdot10^{-9}$, respectively. For the zonal tides with $m = 0$, $\delta\boldsymbol{\Omega}_{\rm loc}$ has only an east-west component, and our choice of a ring laser does not sense these tides.

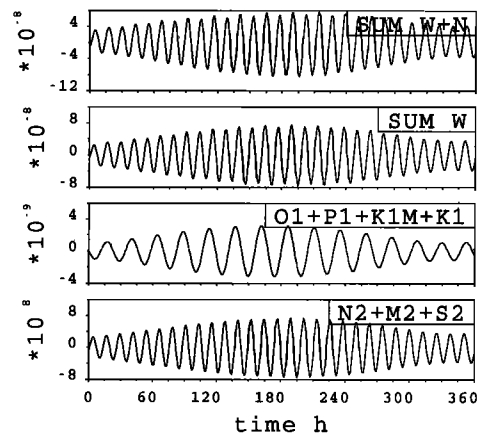

Figure 1. Tidally induced Sagnac effects in a vertical laser at Christchurch, New Zealand from 1 January, 1997 onwards. The diagrams are (from bottom to top): $\delta f_\Omega/f$ for main semi-diurnal constituents, $\delta f_\Omega/f$ for main diurnal constituents, sum of $\delta f_\Omega/f$ for main semi-diurnal and diurnal constituents, sum of $\delta f_\Omega/f$ and $\delta f_n/f$. For an explicit plot of $\delta f_n/f$ see Fig. 2.

Sagnac contribution from tilt

The projection term δf_n is proportional to $\delta\mathbf{n}$ given in Eq. (14). For ring lasers with normals aligned with the coordinate vectors, $\delta\mathbf{n}$ is given by

$$\delta\mathbf{n}_r = \frac{1}{g}\sum_{nmk}\frac{\ell_n - h_n}{R_e}\,\nabla_o\phi_{nmk} \quad (15)$$

$$\delta\mathbf{n}_\vartheta = -\frac{1}{g}\sum_{nmk}\left[\frac{\ell_n - h_n}{R_e}\,\mathbf{e}_r\frac{\partial}{\partial\vartheta} + \frac{im\ell_n}{R_e\sin\vartheta}\,\mathbf{e}_\lambda\left(\frac{\partial}{\partial\vartheta} - \cot\vartheta\right)\right]\phi_{nmk} \quad (16)$$

$$\delta\mathbf{n}_\lambda = -\frac{1}{g}\sum_{nmk}\left[\frac{\ell_n - h_n}{R_e}\,\frac{im}{\sin\vartheta}\,\mathbf{e}_r + \frac{im\ell_n}{R_e\sin\vartheta}\,\mathbf{e}_\vartheta\left(\frac{\partial}{\partial\vartheta} - \cot\vartheta\right)\right]\phi_{nmk} \quad (17)$$

where the index of $\delta\mathbf{n}$ indicates the coordinate direction of $\mathbf{n}_0$ as well as $\mathbf{n}_S$.

For a horizontal laser ($\mathbf{n}_0 = \mathbf{n}_S = \mathbf{e}_r$) at Christchurch, the projection term is of the order of $4\cdot10^{-8}$ and $4\cdot10^{-9}$ for the semi-diurnal and diurnal tides, respectively (Fig. 2). The projection term due to the zonal tides ($m = 0$) is of the order of $6\cdot10^{-9}$, as is illustrated by the largest zonal constituent, the fortnightly tide *Mf*. For a vertical laser with $\mathbf{n}_0 = \mathbf{n}_S = \mathbf{e}_\vartheta$, the projection term is nearly identical to the

[2] Due to inertial forces, these numbers actually are frequency dependent, however, at tidal frequencies this dependency may be neglected.

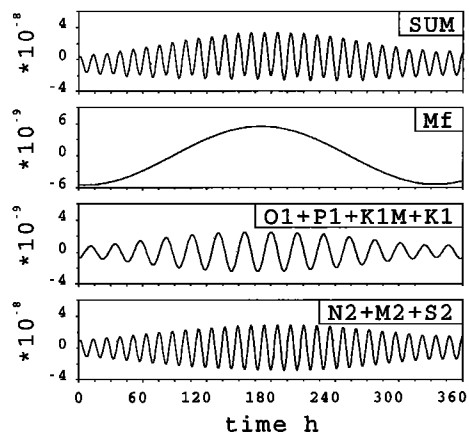

Figure 2. Same as Fig. 1 but for a horizontal laser. The diagrams are (from bottom to top): $\delta f_n/f$ for main semi-diurnal constituents, $\delta f_n/f$ for main diurnal constituents, $\delta f_n/f$ for the main long-period constituent, sum of $\delta f_n/f$ for the main semi-diurnal, diurnal and long-period constituents.

horizontal laser except for a change in sign. In the case of $\mathbf{n}_0 \parallel \boldsymbol{\Omega}$, the projection term vanishes independent of $\mathbf{n}_S$.

Consequences for the detection of tidally induced effect

The detectability only of the projection term shows that a horizontal ring laser acts as a tiltmeter. Particularly for tilting, the Earth's response to tidal forcing may locally be strongly modified compared to the response of the SNREI Earth model used here, with these modifications primarily being due to lateral heterogeneities and the local stress field. Moreover, signals arising from meteorological, oceanic and hydrological loading may exceed the Earth tidal signal by an order of magnitude. Nevertheless, we may expect the C-II ring laser horizontally mounted in a cave 30 m under the surface at Christchurch, New Zealand, and the proposed "G" [Grossring, see *Anderson et al.*, 1994] to give a tidal signal of approximately the form and order of those displayed in Fig. 2 albeit with some cavity effects superimposed, typically a few tens of percent [*Harrison*, 1978].

A ring laser mounted vertically with its area vector $\mathbf{A}$ parallel to $\mathbf{e}_\vartheta$ would detect the vorticity signal given in Fig. 1 with maximal sensitivity, and it would also be sensitive to the projection term. A tilted ring laser with $\mathbf{n}_0 \parallel \boldsymbol{\Omega}$ would be insensitive to the projection term, and hence to the associated cavity effects. This would be the cleanest configuration for detecting the tidal vorticity effect.

Due to the model and reference frame used, $\delta\boldsymbol{\Omega}_{\mathrm{loc}}$ as given here does not contribute to the variation of the global rotation vector $\boldsymbol{\Omega}$, i.e., the global average of $\delta\boldsymbol{\Omega}_{\mathrm{loc}}$ vanishes. At diurnal and semidiurnal frequencies, tides are the dominant signal, and the tidally induced global PM and LOD signals are of the order of 10^{-8} and 10^{-9}, respectively. These signals can be modelled theoretically with high precision [see e.g. *Lambeck*, 1988]. The residual tidal signals are of the order of 10 % of the total signals, and they are thought to result mainly from imperfections of the ocean tide and Earth models [*Herring and Dong*, 1994]. Therefore, $\delta\boldsymbol{\Omega}_{\mathrm{glob}}$ can be modelled with uncertainties being at least an order of magnitude smaller than the local tidal signal. Thus, the tidally induced Sagnac effects both due to tilt and vorticity may prove to be key effects in the validation of the ring laser as a technique for Earth rotation monitoring.

Acknowledgements. We wish to thank H R Bilger, J Müller and U Schreiber for discussions. GES was partially supported by PGSF contract UOC 408, and Marsden Fund contract UOC 513.

References

Anderson, R., H. R. Bilger, and G. E. Stedman, "Sagnac" effect: A century of Earth-rotated interferometers, *Am. J. Phys.*, *62*, 975–985, 1994.

Bilger, H. R., Low frequency noise in ring laser gyros, *Physics of Optical Ring Gyros, Proc. SPIE*, *487*, 42–48, 1984.

Bilger, H. R., G. E. Stedman, Z. Li, U. Schreiber, and M. Schneider, Ring lasers for geodesy, in *IEEE Trans. Instrum. Meas. (special issuefor CPEM/94: Conference on Precision Electromagnetic Measurements, Boulder CO, June 27-July 1, 1994)*, vol. 44, pp. 468–470, 1995.

Dehant, V., J. Hinderer, H. Legros, and M. Lefftz, Analytical approach to the computation of the Earth, the outer core and the inner core rotational motions, *Phys. Earth Planet. Int.*, *76*, 259–282, 1993.

Ducarme, B., Tidal potential developments for precise tidal evaluation, *Bull. Inf. Marées Terrestres*, *104*, 7338–7360, 1989.

Farrell, W. E., Deformation of the Earth by surface loads., *Rev. Geophys. Space Phys.*, *10*, 761–797, 1972.

Harrison, J. C., Implications of cavity, topographic and geological influences on tilt and strain observations, Rept. dept. geod. sci. 280, Ohio State University, 1978.

Hartmann, T., and H.-G. Wenzel, The harmonic development of the Earth tide generating potential due to the direct effect of the planets, *Geophys. Res. Lett.*, *21*, 1991–1993, 1994.

Herring, T. A., and D. Dong, Measurement of diurnal and semidiurnal rotational variations and tidal parameters of earth, *J. Geophys. Res.*, *99*, 18051–18071, 1994.

Hide, R., and J. O. Dickey, Earth's variable rotation, *Science*, *253*, 629–637, 1991.

Lambeck, K., *Geophysical Geodesy - The Slow Deformations of the Earth*, Oxford Science Publications, 1988.

Stedman, G. E., Z. Li, and H. R. Bilger, Sideband analysis and seismic detection in large ring lasers, *Appl. Opt.*, *34*, 7390–7396, 1995.

Wang, R., *Tidal deformations on a rotating, spherically asymmetric, visco-elastic and laterally heterogeneous Earth*, vol. 5 of *European University Studies, Series XVII,Earth Sciences*, Peter Lang, Frankfurt am Main, 1991, 112pp.

Wilhelm, H., Spheroidal and torsional global response functions, *J. Geophys.*, *59*, 16–22, 1986.

Michael Burns and Geoffrey E. Stedman, Dept. of Physics and Astronomy, University of Canterbury, Private Bag 4800, Christchurch, New Zealand

Volker Rautenberg, Hans-Peter Plag and Hans-Ulrich Jüttner, Institut für Geophysik der Christian-Albrechts-Universität zu Kiel, Olshausenstraße 40, D–24118 Kiel, Germany

(received August 1, 1996; revised February 13, 1997; accepted February 23, 1997.)